



**HAL**  
open science

## Multipactor sensitivity to Total Electron Emission Yield and TEEY models accuracy, studies made with a small gap waveguide structure.

Nicolas Fil, Mohamed Belhaj, Julien Hillairet, Jerome Puech

### ► To cite this version:

Nicolas Fil, Mohamed Belhaj, Julien Hillairet, Jerome Puech. Multipactor sensitivity to Total Electron Emission Yield and TEEY models accuracy, studies made with a small gap waveguide structure.. INTERNATIONAL WORKSHOP ON MULTIPACTOR, CORONA AND PASSIVE INTERMODULATION (MULCOPIIM 2017), Apr 2017, NOORDWIJK, Netherlands. hal-03746656

**HAL Id: hal-03746656**

**<https://hal.science/hal-03746656>**

Submitted on 23 Aug 2022

**HAL** is a multi-disciplinary open access archive for the deposit and dissemination of scientific research documents, whether they are published or not. The documents may come from teaching and research institutions in France or abroad, or from public or private research centers.

L'archive ouverte pluridisciplinaire **HAL**, est destinée au dépôt et à la diffusion de documents scientifiques de niveau recherche, publiés ou non, émanant des établissements d'enseignement et de recherche français ou étrangers, des laboratoires publics ou privés.

See discussions, stats, and author profiles for this publication at: <https://www.researchgate.net/publication/315821979>

# Multipactor sensitivity to Total Electron Emission Yield and TEEY models accuracy, studies made with a small gap waveguide structure.

Conference Paper · April 2017

CITATIONS

3

READS

123

4 authors, including:



Nicolas Fil

Centre National d'Etudes Spatiales

27 PUBLICATIONS 76 CITATIONS

SEE PROFILE



Mohamed Belhaj

The French Aerospace Lab ONERA

148 PUBLICATIONS 1,229 CITATIONS

SEE PROFILE

Some of the authors of this publication are also working on these related projects:



ITER Ion Cyclotron Heating and Current Drive System [View project](#)



ITER Robots [View project](#)

# Multipactor sensitivity to Total Electron Emission Yield and TEEY models accuracy, studies made with a small gap waveguide structure.

Nicolas Fil<sup>(1)(2)(3)</sup>, Mohamed Belhaj<sup>(2)</sup>, Julien Hillairet<sup>(1)</sup>, Jérôme Puech<sup>(3)</sup>

<sup>(1)</sup> *CEA-The French Alternative Energies and Atomic Energy Commission  
CEA Cadarache, DRF//IRFM/SI2P/GSCP, 13108 Saint Paul-Lez-Durance, France*

<sup>(2)</sup> *ONERA-The French Aerospace Lab  
ONERA, 31055, France*

<sup>(3)</sup> *CNES-The French National Centre for Space Studies  
CNES, DCT/RF/HT, 31000 Toulouse, France*

## INTRODUCTION

Radio-frequency (RF) antennas and components can be subject to Multipactor effect when used under vacuum conditions [1]. This phenomenon can lead to RF discharges producing undesirable effects inside microwave components. Telecommunication satellite [2], fusion experimental reactors with Tokamak [3] and particle accelerators [4], among other applications, are commonly affected.

The microwave components even under vacuum conditions have free electrons in their environment. The electrons are accelerated by the RF electric field and can impact the components' walls. At this impact, the incident electron (IE) can penetrate the material and then transfer a part of its energy through inelastic interactions. The IE can excite inner material electron which could escape the material surface [5]: in this case the electron emitted is called secondary electron (SE). The IE can also escape the surface material due to several inelastic and elastic interactions: in this case the electron emitted is called backscattered electrons (BSE). We commonly define three yields: the Total Electron Emission Yield (TEEY,  $\sigma$ ) which is the number of the whole electrons emitted by the surface divided by the number of IE, the Secondary-Electron Yield (SEY,  $\delta$ ) which is the number of SE emitted divided by the number of IE and the BackScattered Electron Yield (BSEY,  $\eta$ ) which is the number of BSE emitted divided by the number of IE. The TEEY is the total of the SEY and the BSEY.

Thanks to these definitions, we can now express one main condition for the appearance of Multipactor discharge depends on the electron emission properties of the material. It is needed to get the TEEY higher than unity. It is also necessary to have a resonance between the RF signal and the electron motion. This last condition depends on the geometry of the studied components. In this paper, we use a small gap waveguide structure where the electrons flight time from their emission to the opposite wall has to be an odd number of half periods of the RF signal [6]. When the electron emission and this resonance are both satisfied, an electron cloud grow inside the waveguide. The electron density increase can leads to raise the system noise level and the return loss and arise locally the temperature [7]. The pressure rising, ionization process can also appear driving to corona discharge and electrical breakdowns. Multipactor effect brings many risks to space RF components which can be damaged. In the worst scenario, RF payloads for communication can become unusable. Oversized margins are then applied to avoid it. For fusion reactor application, microwave antenna waveguides as well as RF ceramic feedthroughs can be damaged by multipactor breakdowns. These last components are vacuum barriers and then are critical for the proper functioning and the safety of the fusion reactor. Any damage on RF feedthroughs would lead on air leak and will stop the reactor. Accurate predictions of multipactor thresholds would improve future designs.

Multipactor threshold can be predicted by simulation codes or can be measured by experimental methods. Microwave components are commonly tested and validated with both techniques. Experimentally we can use the third harmonic detection method or the phase nulling [8]. In addition, multipactor simulations codes are used to calculate the threshold that would trigger the electron density growth [9], [10]. A benchmark of different multipactor simulations codes has been made by a multi-laboratory project, showing similar results for multipactor threshold predictions [11]. This uniformity has been found when all multipactor simulation codes used the same TEEY curve and RF structure (small gap waveguide structures). This shows the importance of TEEY data for multipactor predictions. However, when TEEY

model employed to fit representative experimental TEEY data are used in simulations, threshold predictions is questionable.

In this paper, an evaluation of multipactor threshold sensitivity to TEEY curve variations was considered in order to determine TEEY models which are the most suited to be used to predict multipactor threshold. A preliminary study has been published on the proceeding article [12]. Here is presented the complete study showing the whole methodology and providing detailed explanations and simulation results. We study a small gap waveguide structures which is well approximated by a parallel-plate geometry where the RF wave electric field is essentially homogeneous [13]. We choose to study silver material and a capacitive waveguide geometry which allows us to use results from [11]. In the first section, we have collected many electron-emission measurements from which we have extracted two silver TEEY curves representing technical (exposed to atmosphere) and clean (evaporated or ion cleaned under UHV conditions) samples. We also have defined seven regions of interest for a TEEY curve for the purpose of evaluates the multipactor threshold sensitivity to TEEY curve variations. For both clean and technical samples, dispersion of the measurements collected in literature has been extracted for the seven regions of interest. From this results, new TEEY curves have been created and imported inside multipactor simulations with the aim of determine multipactor threshold sensitivity to each TEEY curve region of interest. The multipactor simulation results are presented in the second section. In the third section, six TEEY models are benchmarked with respect to their capability to accurately model these regions.

### CLEAN AND TECHNICAL TEEY CURVES

Hereafter is explained our definition of two silver TEEY curves called references. First, we gathered twenty-seven measurements of silver electron-emission from the sources [14]–[33] collected by Joy [34], as well as data from [11] and our own measurements made on two different silver samples (Associated Dataset available at: <https://doi.org/10.5281/zenodo.154266>) [35]. These data correspond to fourteen backscattered electron yields (BSEY, $\eta$ ), ten secondary electron yields (SEY, $\delta$ ) and three total electron emission yield (TEEY, $\sigma$ ).

By collecting all these data we want to be as representative as possible. Our goal is to extract a TEEY curve called *reference* which describes an average silver TEEY curve with the standard deviation representing by error bars for all electron-emission data. When TEEY data are not available directly from publication, we have calculated it from the addition between averaged BSEY and SEY data. The reference TEEY curve represented on Fig. 1.(a) is the average of all TEEY curves where errors bars correspond to the standard deviations.

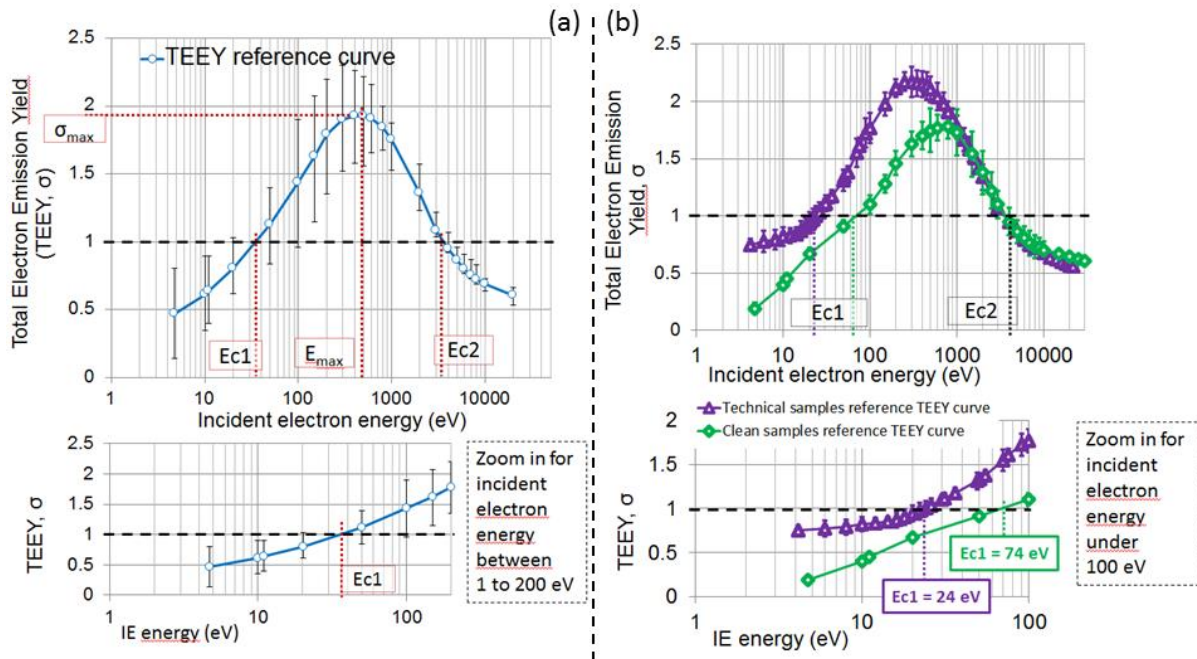


Fig. 1. (a) Average silver TEEY with standard deviations from [11], [14]–[33] and [Associated Dataset available at: <https://doi.org/10.5281/zenodo.154266>] [35]. (b) Technical and clean reference TEEY curves with respective standard deviations. Triangles (technical samples) and diamonds (clean samples).

On the Fig. 1.(a) we see a large deviation, especially for incident electrons energies lower than the maximum energy ( $E_{max}$ ). This characteristic can come from the different sample surface states (*technical* or *clean* samples) or the experimental conditions (temperature, incident electron flux density, and conditioning). All samples are pure silver but the surface sample characteristic varies from one sample to another. Due to the large deviation of this data set, hereafter we distinguish between *technical* and *clean* samples. The difference between the two kinds of samples appears at the surface and the near surface region, technical samples have layers of hydrocarbon compounds while clean samples have not [36]. The presence of such layers near the surface region influence the electron emission because the SE are generated within the first nanometers under the surface material [37]. With the whole literature used [11],[14]–[33] and our own measurements [35], we obtained six and five silver TEEY data series for respectively clean and technical samples. We got both clean and technical reference TEEY curves (Fig. 1.(b)) by using the same methodology presented before.

This paper aims to make an evaluation of multipactor threshold sensitivity to TEEY curve variations. To do so, we define a TEEY curve with seven regions of interest such as: energies under  $E_{c1}$ , energy around the first cross-over  $E_{c1}$ , energies between  $E_{c1}$  and  $E_{max}$ , maximum energy ( $E_{max}$ ), maximum TEEY ( $\sigma_{max}$ ), energies above  $E_{max}$  and energy around the second cross-over  $E_{c2}$ . We apply this definition to both clean and technical reference TEEY curves, which gives the Table 1. It synthesises the description of each of the seven regions of interest and their respective deviations for clean and technical reference TEEY curve from the whole literature used [11],[14]–[33] and our own measurements [35].

Table 1. TEEY curve region of interest and their deviation natures. Both clean and technical samples deviations

TEEY curve regions of interest	Description	Dispersion - [Min - Mean - Max]	
		Clean samples	Technical samples
$E < E_{c1}$	Yield deviation between $E = 0\text{eV}$ and $E_{c1}$	$\pm 0.08$	$\pm 0.095$
$E_{c1}$ (eV)	Energy value of the first cross-over point	[54 - <b>74</b> - 125]	[19 - <b>24</b> - 30]
$E_{c1} < E < E_{max}$	Yield deviation between $E_{c1}$ and $E_{max}$	$\pm 0.19$	$\pm 0.13$
$E_{max}$ (eV)	Energy value of the curve maximum point	[500- <b>800</b> -1000]	[200- <b>250</b> -450]
$\sigma_{max}$	Yield value of the curve maximum point	[1.57- <b>1.78</b> -1.94]	[2.06- <b>2.17</b> -2.30]
$E_{max} < E$	Yield deviation for energies higher than $E_{max}$	$\pm 0.20$	$\pm 0.13$
$E_{c2}$ (eV)	Energy value of the second cross-over point	[2800- <b>3600</b> -4600]	[3200- <b>3600</b> -4100]

To study the multipactor simulation sensibility to TEEY curve variation, regions of interest are tuned one by one. For instance we focus on energy around the first cross-over ( $E_{c1}$ ) for the technical samples. Here,  $E_{c1} \in [19 - 24 - 30]$  with 24 eV the first cross-over mean energy of the technical samples, 19 eV and 30 eV are respectively the lower and higher limit. Thanks to this result, new TEEY curves representing that same deviation are created, the other regions of interests stayed unchanged. These curves only vary around  $E_{c1}$  to be sure to study only one region of interest at a time and then get coherent results from multipactor simulations. Fig. 2 illustrates these created TEEY curves for technical samples and first cross-over region of interest.

We use the identical procedure for the seven regions of interest and for both clean and technical TEEY curves. Seventy-three new TEEY curves have been then created.

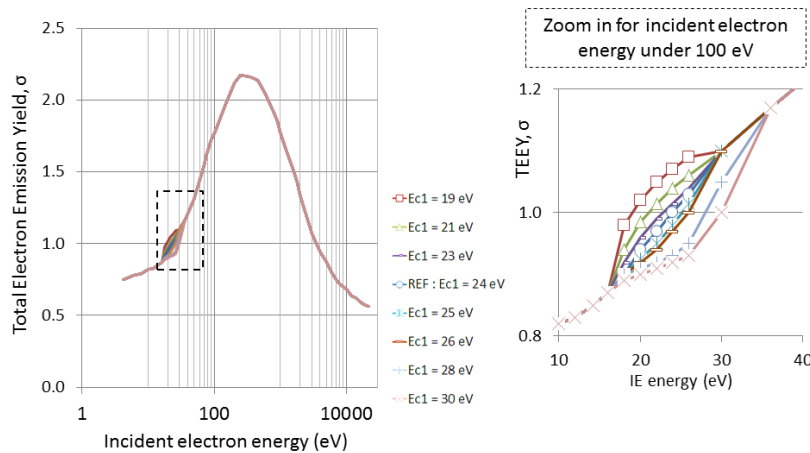


Fig. 2. Representation of variations of first cross-over energy for the technical samples reference TEEY curve obtained from literature deviations.  $E_{c1} \in [19-24-30]$

## MULTIPACTOR THRESHOLD SIMULATIONS SENSITIVITY TO TEEY CURVE VARIATIONS

In [11], a benchmark of multipactor simulation codes demonstrates the consistency of the multipactor threshold predictions when small gap waveguides structures are studied. A 0.10 mm gap Ku-Band waveguide represented in Fig. 3 has been used for this benchmark. This sample has been both simulated and multipactor tested at 12 GHz. Among the codes benchmarked, we choose to use Spark3D software [38] for our study due to its speed simulation time (for this work, more than four hundreds multipactor threshold simulations have been made). Spark3D has been cross-validated with other software and measurements [11]. The same structure has also been cross validated with CST Particle (CST PS) [9] for few TEEY curves.

With Spark3D we can import a TEEY curve; the software will use this data to translate the material electron-emission yield within the multipactor simulation. We also have other parameters to adjust, for all simulations made in this study we use the following parameters: 10,000 initial electrons, no uniform DC magnetic field, and 0.1dB power loop precision. Simulation with Spark3D calculates the multipactor threshold in term of power. In this paper we choose to express the multipactor threshold in term of electric field (with kV/m as unit). To do so, we use the formula (1) to convert the multipactor power breakdown ( $P_{BD}$ ) calculated by Spark3D to multipactor electric field breakdown ( $E_{BD}$ ) [39]. This choice is made with the intention of giving more representative results by taking into account the geometry dimensions within the conversion.

$$P_{BD} = \frac{1}{4} \times \left( \frac{E_{BD}^2 \times k}{\mu_0 \times \omega} \right) \times a \times b \quad (1)$$

with, 
$$k = \sqrt{\left(\frac{\omega}{c}\right)^2 + \left(\frac{\pi}{a}\right)^2} \quad (2)$$

All results express in this paper have been calculated with formulas (1) and (2) from Spark3D multipactor power threshold.

For all TEEY curves created in accordance with the procedure explained in the first section, we made multipactor threshold simulations. With the aim of getting coherent results, for every TEEY curve, we made five strictly identical simulations. After the conversion from the power breakdown to the electric field breakdown, we extract an average threshold value as well as simulations relative errors. This error is up to 1.1% considering the whole simulations made in this study. We obtain an average electric field threshold of  $1878.67 \pm 15.14$  kV/m for clean reference TEEY while for the reference technical TEEY gives an average of  $378.69 \pm 3.06$  kV/m. To determine how the TEEY influence the multipactor threshold, we compared the multipactor simulation results obtained from each newly created TEEY curve with respective reference TEEY. Table 2 synthesis the maximum relative error for the electric field threshold results for each regions of interest and for both clean and technical samples.

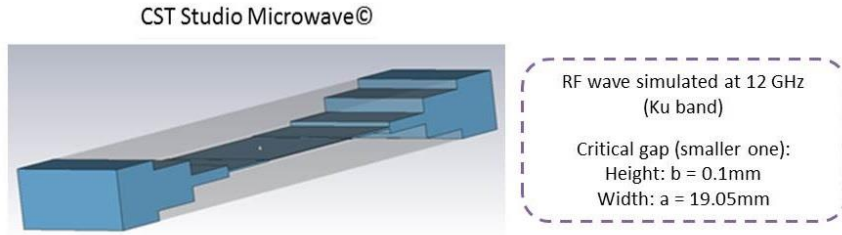


Fig. 3. Ku-Band waveguide simulated during our study. The smallest gap is about 0.1mm and simulations have been performed at 12 GHz. Here is represented the vacuum part of the waveguide used in CST Studio Microwave ©

Table 2 – Multipactor threshold sensitivity to TEEY curve variations

TEEY curve regions of interest	Multipactor simulations results: electric field threshold variations with respective references	
	Clean samples $E_{CLEAN TEEY REF} = 1878.67 \pm 15.14$ kV/m	Technical samples $E_{TECH TEEY REF} = 378.69 \pm 3.06$ kV/m
$E < E_{C1}$	0.78%	0.86%
$E_{C1}$ (eV)	<b>4.13%</b>	<b>2.10%</b>
$E_{C1} < E < E_{max}$	<b>7.13%</b>	<b>4.17%</b>
$E_{max}$ (eV)	0.16%	0.38%
$\sigma_{max}$	0.78%	0.62%
$E_{max} < E$	0.16%	0.62%
$E_{C2}$ (eV)	0.47%	0.14%

From Table 2, we extract two critical regions of interest, the ones which have relative difference above the simulation relative error of 1.1%: first cross-over energy and energies between the first cross-over and the maximum. It means that these two regions of interests have the most influence on multipactor simulation threshold. These results imply that both TEEY measurements and models should be accurate in those two regions.

## TEEY MODELS FOR MULTIPACTOR ACCURATE PREDICTIONS

Multipactor numerical analyses commonly use total electron emission yield (TEEY) models to simulate the response of materials to an incident electron beam. The aim is to be as close as possible of real conditions, when experimental data are not available. Since secondary-electrons are generated near the surface (at a few nanometers depth) [37], electron emission measurements must be performed under representative conditions (vacuum, temperature and surface composition and roughness). Several authors proposed TEEY models. However, a significant spread is generally observed between TEEY models.

In the previous section, it is shown that a suitable TEEY has to be accurate around  $E_{c1}$  and between the first cross-over and the maximum ( $E_{c1} < E < E_{max}$ ) for small gap waveguide structures. In this section, we define a tolerance range for which a TEEY model must be accurate enough to stay under the numerical error of multipactor simulations using this TEEY model. The simulation relative errors have been found to be lower than 1.1% from all simulations made in this study.

The tolerance ranges are focused on the two most relevant TEEY regions of interest:  $E_{c1}$  and  $E_{c1} < E < E_{max}$ . We work with the narrower tolerance ranges without being on simulation noise. Consequently, we choose to work with a simulation precision of 1.1 %.

First, we study the first cross-over energy for the technical samples case. A variation of 1.1% of the technical reference electric field threshold is equivalent to a TEEY curve variation of  $E_{c1}$  of 1 eV. Therefore, TEEY model need to have less than 1 eV variation for  $E_{c1}$  to predict accurate multipactor threshold. A 1eV-standard deviation with the value of 24eV for reference  $E_{c1}$  technical samples is equivalent of 4.2%.

For clean samples case, 1.1% variation of the clean reference electric field threshold is equivalent to a TEEY curve variation of  $E_{c1}$  of 8 eV. This leads to a 10.8% tolerance range on the value of  $E_{c1}$  for TEEY models.

For the second region of interest, the curve points between the first cross-over and the maximum ( $E_{c1} < E < E_{max}$ ) are shifted in ordinate by a certain  $\Delta\sigma$ . The values of  $E_{c1}$  and  $E_{max}$  stay identical to the ones of the reference while the yields between the first cross-over and the maximum are increase or decrease by a  $\Delta\sigma$ .

For technical samples case, a variation of 1.1% of the technical reference electric field threshold is equivalent to a  $\Delta\sigma = \pm 0.07$ . TEEY model need to have less than 4.7% variation between first cross-over and maximum energies to predict accurate multipactor threshold.

For clean samples case, 1.1% variation of the clean reference electric field threshold is equivalent to a  $\Delta\sigma = \pm 0.02$ . This leads to a 1.8% tolerance range between first cross-over and maximum energies for TEEY models.

The four tolerance ranges are synthesis in Table 3.

We aim to evaluate which models are more likely to predict precise multipactor threshold. Thanks to previous tolerance ranges we can now compare TEEY models with respect to reference TEEY. For each TEEY model we fit both clean and technical reference TEEY and extract the respective variations for both critical regions of interest ( $E_{c1}$  and  $E_{c1} < E < E_{max}$ ). If these variations are under tolerance ranges, the TEEY model is able to predict coherent multipactor threshold. The main results are synthesised in Table 4.

Table 3 – Tolerance ranges which have to be respected by TEEY model to be accurate for multipactor threshold simulations

TEEY curve parameters	TEEY model need to respect the following tolerance ranges to give accurate prediction of multipactor threshold simulations	
	Clean samples	Technical samples
$E_{c1}$ (eV)	<b>10.8 % (<math>\pm 8\text{eV}</math>)</b>	<b>4.2 % (<math>\pm 1\text{eV}</math>)</b>
$E_{c1} < E < E_{max}$	<b>1.8 %</b>	<b>4.7 %</b>

Table 4 –TEEY model capabilities to predict multipactor threshold by being or not under tolerance ranges

TEEY models	TEEY model comparison with reference TEEY curves			
	Clean samples		Technical samples	
	$E_{c1}$	$E_{c1} < E < E_{max}$	$E_{c1}$	$E_{c1} < E < E_{max}$
Tolerance ranges	10.8% ( $\pm 8eV$ )	1.8%	4.2% ( $\pm 1eV$ )	4.7%
[40]	19.5%	6.9%	27.4%	13.9%
[41]	110.2%	14.7%	262.5%	45.4%
[42]	0%	1.6%	0%	4.4%
[43]	252.5%	32.3%	164.5%	30.8%
[44]	188.6%	24.2%	115.4%	21.0%
[45]	88.0%	12.1%	23.4%	3.1%

[42] TEEY model can fit precisely enough both clean and technical TEEY to give coherent multipactor threshold predictions. The others five TEEY models are not suited to be used to predict accurate multipactor threshold in small gap waveguide structures like the one studied in this paper.

To illustrate these results and conclusions, we made new simulations importing TEEY from models [40]–[45] in Spark3D. We made simulations with Spark3D parameters previously used in the third section. Five multipactor threshold simulations have been made for each TEEY. Table 5 shows the results extract from these simulations. Then for one TEEY model and one kind of sample (clean or technical), we report the average electric field threshold obtained thanks to the five simulations. In brackets refers the standard deviation in respect with reference average electric field threshold (clean or technical).

Table 5 shows coherence with the results in Table 4, the prediction of the multipactor threshold become more and more inaccurate when TEEY model are more and more imprecise around the first cross-over energy and between the first cross-over and the maximum energies. This commonly leads to predict higher multipactor threshold because the TEEY models give the first cross-over energy at higher values. It is important then to really pay attention on TEEY model and data in order to avoid inaccurate multipactor threshold predictions.

In [46], results from multipactor threshold are presented and our Ku-Band waveguide simulated during this study see a power threshold of 229W (or 389.21kV/m). This multipactor test result can be compared to simulations with technical samples due to the natural presence of a layer of hydrocarbon compounds at the surface and the near surface region. The difference between simulation with  $P_{TECH\ TEEY\ REF} = 217 \pm 3\ W$  (or  $E_{TECH\ TEEY\ REF} = 378.69 \pm 3.06\ kV/m$ ) and test is within +/- 0.17dB and +/- 0.29dB.

Table 5 – Simulated Multipactor electric field threshold with TEEY from models [40]–[45]

Average electric field threshold: clean ref TEEY curve 1878.67±15.14 kV/m; technical ref TEEY curve (378.69±3.06 kV/m).

TEEY models	Multipactor simulations results: threshold electric field for TEEY from models [40]–[45] (and standard deviation relative to clean and technical reference electric field threshold)	
	Clean samples ( $E_{CLEAN\ TEEY\ REF} = 1878.67 \pm 15.14\ kV/m$ )	Technical samples ( $E_{TECH\ TEEY\ REF} = 378.69 \pm 3.06\ kV/m$ )
[40]	1892.40±12.28 kV/m (0.73%)	400.90±1.93 kV/m (5.87%)
[41]	2068.54±14.96 kV/m (10.11%)	1758.49±14.07 kV/m (364.37%)
[42]	1881.46±15.04 kV/m (0.15%)	376.98±2.05 kV/m (0.45%)
[43]	2208.67±9.36 kV/m (17.57%)	636.51±3.25 kV/m (68.08%)
[44]	2164.27±4.28 kV/m (15.20%)	523.34±4.92 kV/m (38.20%)
[45]	2073.52±9.97 kV/m (10.37%)	394.40±1.97 kV/m (4.15%)

## CONCLUSION

This paper explains a methodology to study the influence of TEEY model choice on the simulation of multipactor threshold. Electron emission data for silver material has been collected from numerous references in order to be representative of the literature. We determined that for a small gap waveguide structure, multipactor threshold simulations depend mostly of the first cross-over and the maximum point energies. In order for simulations to get



results close to experimental TEEY data, TEEY model curves need to be accurate in these both regions. Six TEEY models frequently used in multipactor simulations have been benchmarked with respect to their relevance in modeling these two regions of interest of the TEEY curves. For the small gap geometry used, the most relevant TEEY model has been found to be [42]. This work illustrates the importance of the choice of the TEEY model to get relevant multipactor simulations. In this paper the interest is focused on small gap waveguide structure which is closed to a parallel-plate geometry. Therefore, the analyses and the conclusions made here about the sensitivity of the multipactor threshold to the TEEY model remain qualitatively valid. For other kind of waveguide structures where the parallel-plate approximation is no longer valid, the whole methodology presented here should be reproduced [47].

## APPENDIX

[42] TEEY model developed by J. Sombrin in the 90s has been created to be accurate on the first cross-over energy. Between the six TEEY models compared in this paper, it's the only one which directly takes into account the value of  $E_{c1}$  in its formula (4). The TEEY ( $\sigma$ ) is calculated from the formula (3). The results published in [42] have been obtained thanks to the Sombrin TEEY model formed by the formulas (3) and (4).

$$\sigma = \frac{2 \cdot \sigma_{max} \cdot \left(\frac{E_i}{E_{max}}\right)^E}{1 + \left(\frac{E_i}{E_{max}}\right)^{2E}} \quad (3)$$

With,

$$E = \frac{\ln(\sigma_{max} - \sqrt{\sigma_{max}^2 - 1})}{\ln\left(\frac{E_{c1}}{E_{max}}\right)} \quad (4)$$

$E_i$  is the incident electron energy.

## REFERENCES

- [1] J. R. M. Vaughan, "Multipactor," *Electron Devices, IEEE Trans.*, vol. 35, no. 7, pp. 1172–1180, 1988.
- [2] J. de Lara, F. Pérez, M. Alfonso, L. Galán, I. Montero, E. Román, and D. R. Garcia-Baquero, "Multipactor prediction for on-board spacecraft RF equipment with the MEST software tool," *IEEE Trans. Plasma Sci.*, vol. 34, no. 2, pp. 476–484, 2006.
- [3] M. Goniche, C. El Mhari, M. Francisquez, S. Anza, J. H. Belo, P. Hertout, and J. Hillairet, "Modelling of power limit in RF antenna waveguides operated in the lower hybrid range of frequency," *Nucl. Fusion*, vol. 54, no. 1, p. 13003, 2014.
- [4] G. Rumolo, F. Ruggiero, and F. Zimmermann, "Simulation of the electron-cloud build up and its consequences on heat load, beam stability, and diagnostics," *Phys. Rev. Spec. Top. - Accel. Beams*, vol. 4, no. 1, pp. 25–36, 2001.
- [5] M. Rosler, "Theory of Electron Emission from Solids by Proton and Electron Bombardment," vol. 213, pp. 213–226, 1988.
- [6] J. Puech, L. Lapierre, J. Sombrin, V. Semenov, A. Sazontov, M. Buyanova, N. Vdovicheva, U. Jordan, R. Udiljak, D. Anderson, and M. Lisak, "A Multipactor Threshold in Waveguides: Theory and Experiment," in *Quasi-Optical Control of Intense Microwave Transmission*, 2005 Spring., J. L. Hirshfield and M. I. Petelin, Ed. 2005, pp. 305–323.
- [7] A. Neuber, J. Dickens, D. Hemmert, H. Krompholz, S. Member, L. L. Hatfield, M. Kristiansen, and L. Fellow, "Window Breakdown Caused by High-Power Microwaves," *Plasma Sci.*, vol. 26, no. 3, pp. 296–303, 1998.
- [8] R. Udiljak, D. Anderson, P. Ingvarson, U. Jordan, U. Jostell, L. Lapierre, G. Li, M. Lisak, J. Puech, and J. Sombrin, "New method for detection of multipaction," *IEEE Trans. Plasma Sci.*, vol. 31, no. 3, pp. 396–404, 2003.
- [9] G. Romanov, "Update on multipactoring in coaxial waveguides using {CST} Particle Studio," 2011.
- [10] V. E. Semenov, E. I. Rakova, D. Anderson, M. Lisak, and J. Puech, "Multipactor in rectangular waveguides," *Phys. Plasmas*, vol. 14, no. 3, pp. 1–8, 2007.
- [11] J. Puech, C. E. Miquel-Espana, and D. Raboso, "Synthesis of the results of the EVEREST project," *Proc. MULCOPIM 2014*, no. 1, 2014.
- [12] N. Fil, M. Belhaj, J. Hillairet, and J. Puech, "Multipactor threshold sensitivity to Total Electron Emission Yield in parallel-plate waveguide and TEEY models accuracy," *IEEE Int. Microw. Symp.*, no. 1, pp. 2–5, 2016.
- [13] E. Sorolla and M. Mattes, "Multipactor saturation in parallel-plate waveguides," *Phys. Plasmas*, vol. 19, no. 7, pp. 1–10, 2012.
- [14] H. E. Bishop, "PhD Thesis," University of Cambridge, 1963.

- [15] R. Böngeler, U. Golla, and M. Kässens, L. Reimer, B. Schindler, R. Senkel, M. Spranck, M. Kässens, L. Reimer, B. Schindler, R. Senkel, M. Spranck, and M. Kässens, L. Reimer, B. Schindler, R. Senkel, M. Spranck, P. Institut, and E. Scattering, "Electron-Specimen Interactions in Low-Voltage Scanning Electron Microscopy," *Scanning*, vol. 15, no. 1, pp. 1–18, 1993.
- [16] I. M. Bronstein and B. S. Fraiman, *Vtorichnaya Elektronnaya Emissiya*, Nauka. Moscow, 1969.
- [17] H. Bruining and J. M. De Boer, "Physica V," 1938, p. 17.
- [18] V. E. Cosslett and R. N. Thomas, "Multiple scattering of 5-30 keV electrons in evaporated metal films: I. Total transmission and angular distribution," *Br. J. Appl. Phys.*, vol. 15, no. 8, pp. 883–907, 2002.
- [19] H. Drescher, L. Reimer, and Z. Seidel, "Backscattering and secondary electron emission of 10-100 keV electrons in scanning electron microscopy," in *Angew Physik 29*, 1970, pp. 331–336.
- [20] A. Assa'd and M. El Gomati, "Backscattering Coefficients for Low Energy Electrons," *Scanning Microsc.*, vol. 12, no. 1, p. 185, 1998.
- [21] K. F. J. Henrich, "Electron probe microanalysis by specimen current measurement," in *Proc. 4th Conf. on X-ray Optics and Microanalysis*, 1966, p. 159.
- [22] H.-J. Hunger and L. Kuchler, "Measurements of the electron backscattering coefficient for quantitative EPMA in the energy range of 4 to 40 keV," *Phys. Status Solidi*, vol. 56, no. 1, pp. K45–K48, 1979.
- [23] K. Kanaya and S. Okayama, "Penetration and energy-loss theory of electrons in solid targets," *J. Phys. D. Appl. Phys.*, vol. 5, no. 1, pp. 43–58, 1972.
- [24] K. Kanaya and S. Ono, "Interaction of electron beam with the target in SEM," in *Electron Beam Interactions with Solids*, SEM Inc., A. O'Hare, Ed. 1984, pp. 69–98.
- [25] D. A. Moncrieff and P. R. Barker, "Secondary electron emission in the scanning electron microscope," *Scanning 1*, pp. 195–197, 1978.
- [26] H. P. Myers, "The Secondary Emission from Copper and Silver Films Obtained with Primary Electron Energies below 10 eV," *Proc. Roy. Soc. L. A.*, vol. 215, no. 1122, pp. 329–345, 1952.
- [27] G. Neubert and S. Rogaschewski, "Backscattering coefficient measurements of 15 to 60 keV electrons for solids at various angles of incidence," *Phys. Status Solidi*, vol. 59, no. 1, pp. 35–41, 1980.
- [28] P. Palluel, "Backscattered components of electron secondary emission from metals," *Compt. Rend. Acad. Sci.*, vol. 224, pp. 1492–1494, 1947.
- [29] J. Philibert and E. Weinryb, "The use of specimen current in electronprobe microanalysis," in *Proc. 3rd Conf on X-ray Optics and Microanalysis*, 1963, pp. 451–476.
- [30] L. Reimer and C. Tollkamp, "Measuring the backscattering coefficient and secondary electron yield inside a scanning electron microscope," *Scanning*, vol. 3, no. 1, pp. 35–39, 1980.
- [31] R. Shimizu, "Secondary electron yield with primary electron beam of kilo-electron-volts," *J. Appl. Phys.*, vol. 45, no. 5, pp. 2107–2111, 1974.
- [32] N. R. Whetten, "Methods in Experimental Physics IV," *Acad. Press New York*, vol. 4, 1962.
- [33] D. B. Wittry, "Secondary electron emission in the electron probe," in *Proc. 4th Conf. on X-ray Optics and Microanalysis*, 1966, pp. 168–180.
- [34] D. C. Joy, "web.utk.edu/~srcutk/database.doc," *University of Tennessee*. .
- [35] M. Belhaj and T. Gineste, "ONERA silver TEEY measurements," *Zenodo*, 2014. [Online]. Available: <https://doi.org/10.5281/zenodo.154266>.
- [36] T. Gineste, M. Belhaj, G. Teyssedre, and J. Puech, "Investigation of the electron emission properties of silver: From exposed to ambient atmosphere Ag surface to ion-cleaned Ag surface," *Appl. Surf. Sci.*, vol. 359, pp. 398–404, 2015.
- [37] A. Shih, J. Yater, C. Hor, and R. Abrams, "Secondary electron emission studies," *Appl. Surf. Sci.*, vol. 111, pp. 251–258, 1997.
- [38] J. Perez, "High Power Analysis in Coaxial Combline Resonator Filters," *fest3d.com/papers.php*. .
- [39] M. Francisquez, "Power Limit Modeling of Lower Hybrid Antenna Waveguides in Tokamaks," Dartmouth College, Hanover, NH, 2012.
- [40] G. F. Dionne, "Origin of secondary-electron-emission yield-curve parameters," *J. Appl. Phys.*, vol. 46, no. 8, pp. 3347–3351, 1975.
- [41] R. G. Lye and A. J. Dekker, "Theory of secondary emission," *Phys. Rev.*, vol. 107, no. 4, pp. 977–981, 1957.
- [42] J. Sombrin, "CLAQUAGE HYPERFRÉQUENCE ET EFFET MULTIPACTOR DANS LES SATELLITES," *OHD93, Publ. results have been obtained with Sombrin TEEY Model*, 1993.
- [43] B. K. Agarwal, "Variation of Secondary Emission with Primary Electron Energy," in *Proc. Phys. Soc.*, 1958, vol. 71, pp. 851–852.
- [44] H. Seiler, "Secondary electron emission in the scanning electron microscope," *J. Appl. Phys.*, vol. 54, no. 11, pp. 1–18, 1983.
- [45] J. Rodney and M. Vaughan, "A New Formula for Secondary Emission Yield," *IEEE Trans. Electron Devices*, vol. 36, no. 9, pp. 1963–1967, 1989.
- [46] P. Mader, C. Feat, J. Lafond, P. Lepeltier, and J. Puech, "TAS-F activities in EVEREST project: results and comments," *Proc. MULCOPIM 2014*, no. 1, 2014.
- [47] H. Bruining and J. H. De Boer, "Secondary Electron Emission - Part I. Secondary Electron Emission of Metals," *Physica*, vol. 5, no. 1, pp. 17–30, 1938.